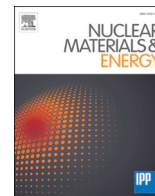


# Theoretical calculation of cesium deposition and co-deposition with electronegative elements on the plasma grid in negative ion sources

journal or publication title	Nuclear Materials and Energy
volume	34
number	March 2023
page range	101334
year	2022-12-06
NAIS	13691
URL	<a href="http://hdl.handle.net/10655/00013534">http://hdl.handle.net/10655/00013534</a>

doi: <https://doi.org/10.1016/j.nme.2022.101334>





## Theoretical calculation of cesium deposition and co-deposition with electronegative elements on the plasma grid in negative ion sources

Heng Li<sup>a</sup>, Xin Zhang<sup>a,\*</sup>, Yuhong Xu<sup>a,\*</sup>, Guangjiu Lei<sup>b</sup>, Katsuyoshi Tsumori<sup>c</sup>, Mitsutaka Isobe<sup>c</sup>, Akihiro Shimizu<sup>c</sup>, Zilin Cui<sup>a</sup>, Yiqin Zhu<sup>a</sup>, Jun Hu<sup>a</sup>, Yuxiang Ni<sup>d</sup>, Shaofei Geng<sup>b</sup>, Haifeng Liu<sup>a</sup>, Xianqu Wang<sup>a</sup>, Jie Huang<sup>a</sup>, Hai Liu<sup>a</sup>, Jun Cheng<sup>a</sup>, Changjian Tang<sup>a,e</sup>, CFQS team<sup>a,c</sup>

<sup>a</sup> Institute of fusion science, School of Physical Science and Technology, Southwest Jiaotong University, Chengdu, 610041, People's Republic of China

<sup>b</sup> Southwestern Institute of Physics, Chengdu, 610041, People's Republic of China

<sup>c</sup> National Institute for Fusion Science, National Institutes of Natural Science, Toki, 5095259, Japan

<sup>d</sup> School of Physical Science and Technology, Southwest Jiaotong University, Chengdu, 610041, People's Republic of China

<sup>e</sup> School of Physical Science and Technology, Sichuan University, Chengdu, 610041, People's Republic of China

### ARTICLE INFO

#### Keywords:

Work function  
Cs covered surface  
Negative ion source  
NBI

### ABSTRACT

We studied the work function of cesium deposition and co-deposition with the electronegative element on the plasma grid (PG) using the first-principles calculations. The impurity particles may exist in the background plasma and vacuum chamber wall, and the work function of the PG will be affected. The results indicate that the minimum work functions of pure cesium deposition on Mo (110), W (110), and Mo (112) are reached at a partial monolayer. They are 1.66 eV ( $\sigma = 0.56 \theta$ ), 1.69 eV ( $\sigma = 0.75 \theta$ ), and 1.75 eV ( $\sigma = 0.88 \theta$ ), respectively. An appropriate co-deposition model consisting of cesium with electronegative elements can further decrease the work function. The coverage of cesium and electronegative elements are both 0.34  $\theta$  in all the co-deposition models. The F-Cs co-deposition model where the Cs atom and F atom are aligned along the surface normal obtains the lowest work function. They are 1.31 eV for F-Cs on Mo (110), and 1.23 eV for F-Cs on W (110), respectively. The change in work function is linearly related to the change in dipole moment density with a slope of  $-167.03 \text{ V\AA}$ . For pure cesium deposition, two factors control the change in dipole-moment density, one is the electron transfer between adsorbates and the substrate, and another one is the restructuring of surface atoms. There are two additional factors for the co-deposition model. One is the intrinsic dipole moment of the double layer, the other is the angle between the intrinsic dipole moment and the surface. The latter two factors play important roles in increasing the total dipole moment.

### 1. Introduction

Neutral beam injection (NBI) based on negative hydrogen ion acceleration is one of the most important facilities to heat the magnetic confinement fusion plasma and drive the plasma current [1,2]. Cesium (Cs) injection is an efficient way to enhance the extracted current in a negative ion source [3,4]. This method is the so-called 'surface production', and another is the 'volume production' [3]. The mechanism of surface production has been investigated by many theoretical and experimental works, which show the formation of a lower work function surface by depositing cesium atoms on the plasma grid (PG) contributes to the production of negative hydrogen ions [5–7]. The change in work function is not monotonic with the increasing cesium deposition. The

work function decreases sharply at the beginning and reaches the minimum when the coverage,  $\sigma$ , of Cs is below one monolayer. As reported in [4], the maximum negative ion conversion efficiency is reached where the work function is minimum. Finally, the work function will tend to be saturated with the further increase of cesium [8,9]. Some theoretical work has been done by Damone et al. [10] and Rutigliano et al. [11]. Damone et al. researched the microstructure of Cs deposition on Mo (100) based on DFT and Molecular Dynamics (MD). They reported the interaction between the Cs atom and the Mo atom using the simple Lennard-Jones type interaction potential. A surface structure of  $\sim 0.7$  layers coverage of Cs on Mo (100) is determined at  $T = 450 \text{ K}$ . Based on the result of Damone et al., Rutigliano et al. researched the H atom scattering from the cesiated surface using DFT and MD. They have given

\* Corresponding authors.

E-mail addresses: [xzhang@my.swjtu.edu.cn](mailto:xzhang@my.swjtu.edu.cn) (X. Zhang), [xuyuhong@swjtu.edu.cn](mailto:xuyuhong@swjtu.edu.cn) (Y. Xu).

<https://doi.org/10.1016/j.nme.2022.101334>

Received 30 September 2022; Received in revised form 1 December 2022; Accepted 4 December 2022

Available online 6 December 2022

2352-1791/© 2022 The Authors. Published by Elsevier Ltd. This is an open access article under the CC BY-NC-ND license (<http://creativecommons.org/licenses/by-nc-nd/4.0/>).

a Mo ( $5 \times 5$ ) surface unit cell ( $A = B = 18.74 \text{ \AA}$ ) and 10 Cs atoms adsorbed. The coverage is  $\sim 0.59$  layers, and the work function of caesiated surface has been calculated (1.81 eV).

Langmuir et al. first noticed this phenomenon and introduced a dipole model to explain it [7]. According to the dipole model, one cesium atom is assumed to lose its outmost single electron and then become a positive cesium ion. Naturally, the metal substrate, molybdenum or tungsten [3], is negatively charged. So a dipole is formed between the adsorbate and substrate. In the work of Singh et al. [12], a phenomenological model has been reported. The decreasing work function  $\Delta\phi$  is derived from the work done by the electric field on the electron,  $\Delta\phi = \mathbf{E} \cdot \mathbf{ed} = \mathbf{E} \cdot \mathbf{p} = Epcos(\beta)$ , where  $d$  is the distance between adsorbate and substrate,  $e$  is the elementary charge,  $\mathbf{p} = \mathbf{ed}$  is the dipole moment, and  $\beta$  is the effective angle, made by the dipole axis with respect to surface normal. This model can intuitively explain why the electrons can escape from the surface more easily. The work function is the minimum barrier that an electron has to overcome to escape, which is affected by the magnitude and direction of the dipole moment. In this phenomenological model, the distribution of electrons is deterministic and discontinuous, at least for the dipole. The amount of charge transferred between the adatoms and the substrate is also deterministic; for example, a Cs atom will transfer an electron to the surface in this model. Many complex factors, such as the interaction between electrons and surface relaxations caused by adatoms, are not considered.

This phenomenological model contributes to our understanding of the physical mechanism behind the phenomenon. There, however, are still some classical and inappropriate assumptions. According to quantum mechanics and density functional theory (DFT), the distribution of electrons is continuous and expressed in terms of electron density. The dipole moment should be  $\mathbf{p} = \int z\rho_e(z)dz$  in a continuously distributed electron gas. The situation will be more complex for different kinds of the multispecies adsorption system. The accurate treatment of this system requires a precise theoretical calculation based on DFT [13,14]. The DFT calculation based on numerical solution still needs to divide the cell into finite-volume elements. Three parameters will control the number of grid-points in the direction of the three lattice-vectors. Therefore, the charge distribution calculated by numerical solution is not continuous, either.

In negative ion sources, a non-ignorable deposition model that hydrogen atoms will co-adsorption with cesium on the PG surface should be noted due to the ubiquitous hydrogen particle during the plasma discharge. In addition to hydrogen, other impurities, such as  $\text{H}_2\text{O}$ , hydrocarbon, and  $\text{O}_2$ , can be easily emitted from the walls of the neutral beamline during plasma discharge and beam acceleration. Additional elements such as oxygen or carbon would be introduced [15–18]. These unavoidable impurities may cause great uncertainty to the performance of the negative ion source. They will be ionized and impact the caesiated surface or the chamber wall with certain energy due to the background plasma temperature and plasma sheath [15]. If the ionization occurs downstream of the extraction electric field, the energetic backstream positive ions will be produced [16]. These ionized particles will deposit on the surface or sputter out surface atoms dependent on their energy. Both deposition and sputtering will affect the surface work function.

Some experimental works indicated that additional hydrogen or oxygen co-deposition with Cs could further decrease the work function [19–21]. The co-adsorption model consists of electronegative and electropositive layers, and the cesium is always on the up-layer [19,20]. The charge transfer and surface structure will be extremely complex in this model and taken for granted causing a double dipole layer in comparison to pure cesium adsorption. Therefore, a quantum mechanics computation that gives theoretically an ideal surface model and precise electron distribution is necessary and pressing.

In this work, we are concerned that these particles are deposited on the surface and completely relaxed. A large number of the adsorbates

deposited on various substrates are studied using the first-principles calculations based on density functional theory (DFT). The monolayer,  $\theta = 1$ , corresponds to a surface-atom density of  $4.8 \times 10^{14} \text{ cm}^{-2}$  [22,23] in this work. In section 2, the computation details and analysis methods are described. In section 3, the simulation and analysis results will be described. Section 3.1 for pure cesium deposition and section 3.2 for cesium co-deposition with impurities. Finally, section 4 is the summary.

## 2. Computational methods

For this calculation work, the Vienna *ab-initio* simulation package (VASP) [24] based on density functional theory (DFT) is used with the local density approximation (LDA) [25] for the exchange–correlation functional. Compared with the generalized gradient approximation (GGA) [26], LDA is better for work function calculation. The projector augmented wave (PAW) [27] method with a cutoff energy of 650 eV is used to describe the ionic core. The tetrahedron method with Blöchl corrections [28] is used and it requires dense k-points, so the  $\Gamma$  centered Monkhorst-Pack scheme [29] with k-points of  $4 \times 4 \times 1$  is adopted by all calculations. All the two-dimensional systems are modeled by using supercell approximation with a vacuum space of 25  $\text{\AA}$  along the z-axis to ensure the electrostatic potential is convergent. The atomic positions and the cell are fully optimized with the convergence criterion that the calculations will be continued up until the force acting each atom becomes less than  $0.02 \text{ eV \AA}^{-1}$ .

As shown in Fig. 1, three kinds of surfaces are used to research the relationship between the work function of PG and cesium coverage, they are Mo (110), W (110), and Mo (112), respectively. Mo and W are excellent candidate materials for PG manufacturing, and their (110) surfaces have a very high intrinsic work function. On the contrary, Mo (112) surfaces have an extremely low intrinsic work function [30]. The sizes of the slab for all surfaces are  $4 \times 4$  with 6 layers and the nethermost two layers are frozen. A smaller ( $3 \times 3$ ) with 6 layers slab is used to calculate the double layers adposition, as shown in Fig. 2. Two kinds of double layers models are taken into account. They are Fig. 2 (a) where the cesium atom and the electronegative species are aligned along the

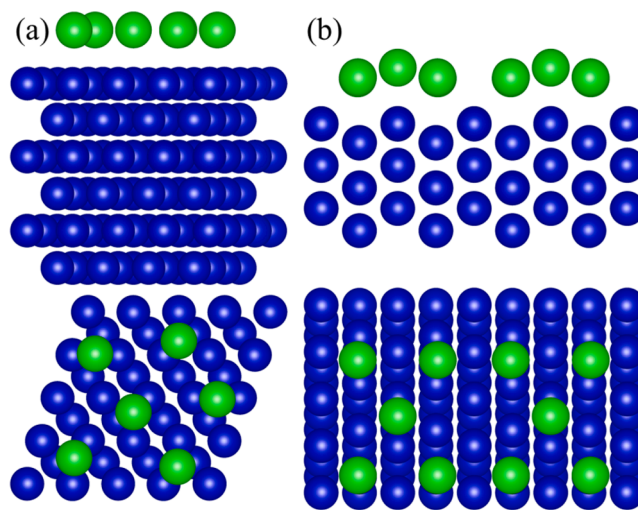


**Fig. 1.** The diagrammatic drawing of cesium atoms deposition on a) Mo/W (110) surface; b) Mo (112) surface. The green atom represents cesium and the blue atom represents molybdenum or tungsten for a) and molybdenum only for b). The coverage  $\sigma$  of cesium in this figure is: a)  $1.13 \theta$  for molybdenum and  $1.12 \theta$  for tungsten, respectively; b)  $1.10 \theta$  for molybdenum only. A different  $\sigma$  determines a different surface structure, especially for the positions of cesium deposition. There is just a slight difference between the Mo (110) surface and W (110) surface, but we just give one picture of Mo (110) to represent them all for reasons of space. (For interpretation of the references to colour in this figure legend, the reader is referred to the web version of this article.)

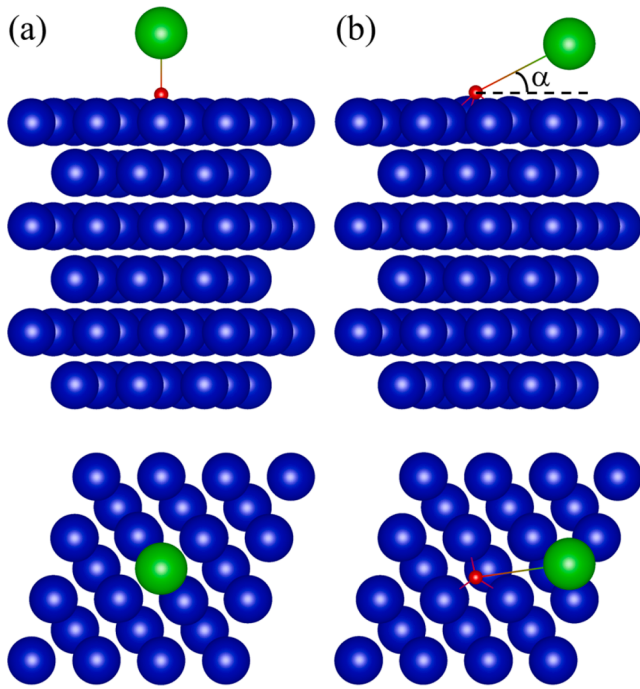


**Fig. 2.** The diagrammatic drawing of cesium atoms co-deposition on Mo (110)/W (110) with the electronegative element. The green atom represents cesium, the blue atom represents molybdenum or tungsten, and the red atom represents H/C/O/F. a), the bonds H-Cs, C-Cs, O-Cs, and F-Cs are perpendicular to the slab; b), the angle between the bonds and slab is  $\alpha$  and shows a state of tilt. Different electronegative element and different slab determines a different structure, we just use the Mo-O-Cs model to represent them all for reasons of space. These models are almost the same as models a) or b), except C-Cs perpendicular to the Mo slab. (For interpretation of the references to colour in this figure legend, the reader is referred to the web version of this article.)

surface normal, and Fig. 2 (b) where the cesium atom and the electronegative species are not aligned along the surface normal, respectively. The difference between these two surface structures stems from the different initial unoptimized structures. In the beginning, we first prepared an optimized surface as the substrate. And then an electronegative atom is placed on the substrate. For the structure of Fig. 2 (a), the cesium atom is placed at the top of the electronegative atom, that is they have the same initial  $x$  and  $y$  coordinates. Only the  $z$  coordinates of the cesium atom and the electronegative species changed after the geometry optimization. They are still aligned along the surface normal. For the structure of Fig. 2 (b), on the contrary, a minor change was made to the initial  $x$  coordinates of the cesium and resulting in a  $\sim 0.1$  Å horizontal distance between these two atoms. The cesium atom and the electronegative atoms are no longer aligned along the surface normal after geometry optimization. Generally, the model Fig. 2 (b) is more stable than a), except for the Mo-C-Cs system in this work.

The work function is the difference between vacuum electrostatic potential and Fermi energy. As said above, the change in dipole moment density will induce a change in work function. Leung et al. [13] combined the dipole moment density  $p = \int_{z_0}^{c/2} z \rho_t(z) dz$  with Poisson equation  $\nabla^2 V = -\rho/\epsilon_0$ , and derived a mathematical expression relating the change in the work function and the change in the surface dipole moment density,  $\phi - \phi_0 = -180.95(p - p_0)$ , where  $z_0$  and  $c/2$  are a point deep inside the slab and the center of the vacuum respectively.  $\phi_0$  ( $\phi$ ) and  $p_0$  ( $p$ ) are the work function and dipole moment density of the clean (contaminative) surface, respectively.  $\rho_t(z) = (1/A) \int_0^{a_1} dx \int_0^{a_2} dy \rho(x, y, z)$ , is the total surface charge density, and  $A$  is the cell surface area.

The surface average electron density difference  $\Delta\rho(z) = \rho(z) - [\rho_s(z) + \rho_a(z)]$ , indicating the charge transfer between the slab and

the adsorbates, where  $\rho(z)$ ,  $\rho_s(z)$ , and  $\rho_a(z)$  are the surface average electron density of the adsorption system, the surface average electron density of the slab, which is generated by removing adsorbates from the slab, and the surface average electron density of adsorbates, respectively. The change in dipole moment induced by the electron density difference is  $\Delta p = \int_{z_0}^{c/2} z \Delta\rho(z) dz = \int_{z_0}^{c/2} z \{\rho(z) - [\rho_s(z) + \rho_a(z)]\} dz = p - (p_s + p_a)$ , and then  $p - p_0 = (p_s - p_0) + p_a + \Delta p$ . So, at least three factors control the total dipole moment density: (i) the charge transfer between surface and adsorbates; (ii) the restructuring of the surface atoms; (iii) the intrinsic dipole moment of adsorbates [13].

### 3. Results and discussions

#### 3.1. Cesium deposition

We studied the cesium cover on the same materials with different index surfaces and the same index surface with different materials at the first. Cesium deposition was widely used in many fields. In the fusion engineering field, cesium is mainly applied to cover the PG electrode, reduce its work function, and then enhance the production efficiency of negative hydrogen ions. As shown in Fig. 3, the tendencies of the work function of cesium atoms deposition on Mo (110), W (110), and Mo (112) are similar. The work function of bare Mo (110), W (110), and Mo (112) are 4.86 eV, 5.13 eV, and 4.44 eV, respectively. They are close to the data in the CRC Handbook of Chemistry and Physics (4.95 eV for Mo (110), 5.22 eV for W (110), and 4.36 eV for Mo (112)) [30]. The lowest work function in these three cases are 1.66 eV ( $\sigma = 0.56 \theta$ ), 1.69 eV ( $\sigma = 0.75 \theta$ ), and 1.75 eV ( $\sigma = 0.88 \theta$ ), respectively. It suggests that the lowest work function of a partial monolayer of cesium deposition is related to the original surface index and materials. However, an original lower work function of the bare surface not always means a lower work function of a partial monolayer of cesium deposition. The lowest work function of Mo (110) and W (110) are almost the same. The mechanics behind this is the change of dipole moment, and we will discuss it below. The fitting curves with polynomial function with the order of 4,  $\phi = a \times \sigma^4 + b \times \sigma^3 + c \times \sigma^2 + d \times \sigma + \phi_0$ , are plotted as an eye guide as shown in Fig. 3. Coefficients are listed in Table 1. As we said before, Rutigliano et al. reported the work function 1.81 eV at  $\sigma = 0.59 \theta$  [11], and we calculated the work function at  $\sigma = 0.59 \theta$  for Mo(110), W(110), and Mo (112) using the fitting formula, respectively. They are 1.67 eV, 1.84 eV, and 1.93 eV respectively. The results are in good agreement.

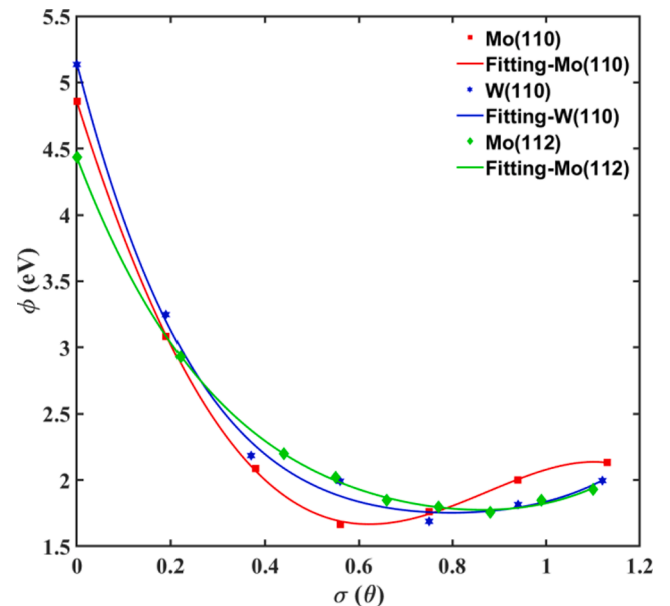


**Fig. 3.** The work function as a function of the coverage  $\sigma$ .

**Table 1**  
The polynomial coefficients.

Surface	$a$	$b$	$c$	$d$	$\phi_0$
Mo (110)	-2.65	0.59	10.58	-11.30	4.86
W (110)	5.14	-16.62	22.02	-13.85	5.14
Mo (112)	3.26	-9.80	13.20	-9.27	4.43

As mentioned above, the slope should be 180.95 VÅ theoretically. Nevertheless, this is an ideal situation cause the Fermi level is set to a constant for all models during the derivation. The shift of the Fermi level should be taken into account for a 2D slab due to its finite thickness [14]. The shift sometimes could be beyond 1.0 eV in this work. In Fig. 4, the negative  $\phi - \phi_0$  values correspond to the decrease of work function induced by an increased dipole moment along the z-axis. After linear fitting of these scattered points, a curve with a slope of 167.03 VÅ is obtained. This difference in slope attributes to the shift of the Fermi level. There is a good linear relation between  $\phi - \phi_0$  and  $p - p_0$ , which means that the change in work function and the change in dipole moment are inextricably linked.

As shown in Fig. 5, the change tendencies of  $p - p_0$  and  $\Delta p$  of the Mo-Cs system are the same, and the maximum is reached at  $\sigma = 0.56 \theta$  where the minimum work function is reached. In the whole process of increasing the dipole moment along the z-axis,  $\Delta p$  always plays a decisive role, with the contribution of  $p_a$  being zero and the contribution of  $p_s - p_0$  being negative. We can conclude that the electron transfer is first increased and then inhibited with the increasing coverage of cesium. It explains the phenomenon that the work function reaches the minimum in the partial monolayers and is finally convergent[3]. To show more details, we plotted Fig. 6 and Fig. 7 including  $p - p_0$ ,  $p_s - p_0$ ,  $p_a$ ,  $\Delta p$ , and the electron density along the z-axis for  $\sigma = 0.19 \theta$  and for  $\sigma = 0.56 \theta$ , respectively. The coverage with  $0.56 \theta$  has a larger total dipole moment than  $0.19 \theta$ , which means a lower work function as shown in Fig. 3. The increment of dipole moment induced by surface atoms restructuring ( $p_s - p_0$ ) is ignorable for both cases because the changes in the position of the surface atom caused by these deposited atoms are extremely limited. Similarly,

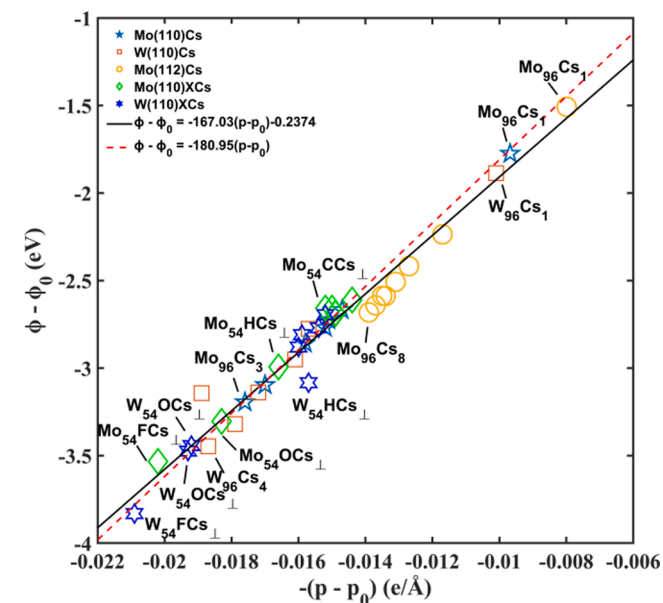


**Fig. 4.** The change in work function plotted as a function of the change in dipole moment density induced by adsorbates. The X represents H, C, O, or F. The black solid line with a slope of 167.03 VÅ is a fitting curve by fitting scatter points. Some surface structures are marked by corresponding indexes. For example, Mo<sub>96</sub>Cs<sub>1</sub> means that the computational model includes 96 Mo atoms as the surface and 1 Cs atom as the adsorbate.

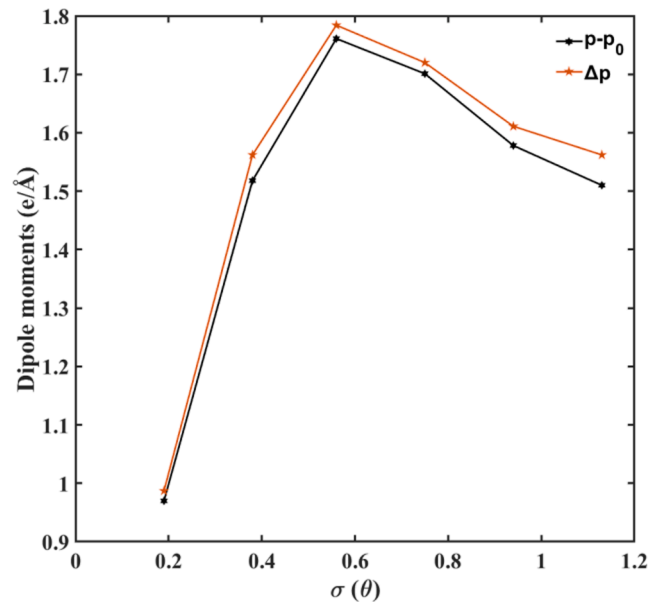


**Fig. 5.** The  $p - p_0$  and  $\Delta p$  as a function of the coverage  $\sigma$  in the system of Mo (110) covered by Cs.

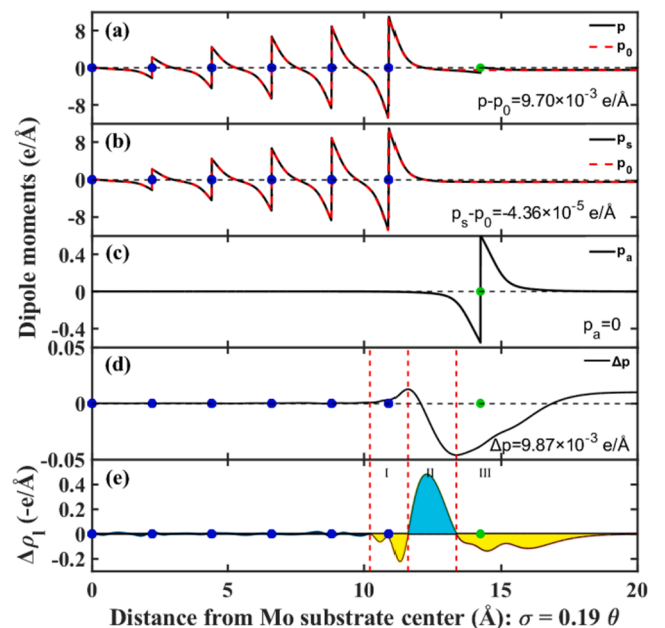


**Fig. 6.** (a) The dipole moment density ( $p$ ) of the “contaminative” Mo (110) surface and the dipole moment density ( $p_0$ ) of clean Mo (110) surface, blue atoms represent the Mo layer, and green atoms represent cesium atoms. (b) The dipole moment density ( $p_s$ ) of unrelaxing Mo (110) surface and  $p_0$ . (c) The intrinsic dipole moment of ( $p_a$ ) adsorbates. (d) The dipole moment density ( $\Delta p$ ) is due to electron transfer between adsorbates and the surface. (e) the electron density difference along the z-axis, the space near the surface is divided into 3 zones by the red dashed line, the yellow regions (I and III) represent electron depletion and the cyan region (II) represents electron accumulation. (For interpretation of the references to colour in this figure legend, the reader is referred to the web version of this article.)

all cesium atoms are at the same height due to the small number of adsorbates, so there is no polarization along the z-axis and then no extra dipole moment ( $p_a = 0$ ). So the main difference is the amount of electron transfer. Fig. 6 (d) shows that the  $\Delta p$  is a positive value preferring to decrease the work function. The magnitude and tendency of  $\Delta p$  are

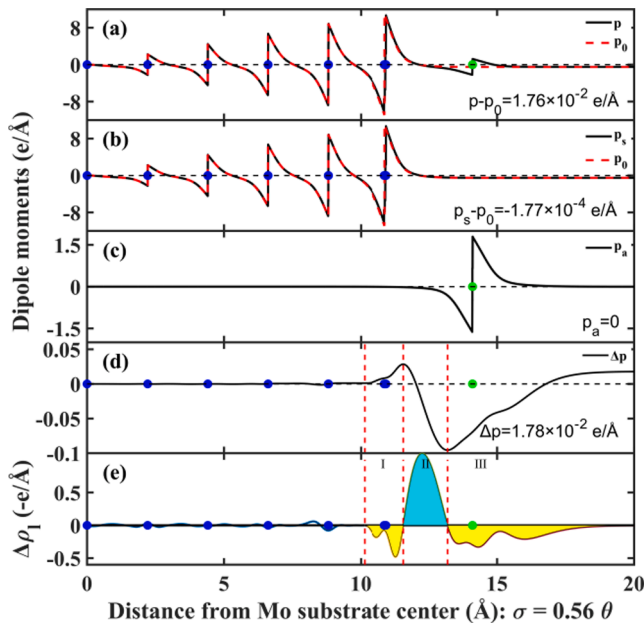


Fig. 7. The same as Fig. 6 but for  $\sigma = 0.56 \theta$ .

determined by the electron transfer in (e) of Fig. 6 and Fig. 7. In the yellow region of the lowest graph,  $\Delta p$  always increases monotonically. On the contrary,  $\Delta p$  always decreases monotonically in the cyan region. A larger magnitude of region I is not effective to increase the dipole moment along the z-axis due to electron conservation. We prefer region III has a larger magnitude to increase the dipole moment along the normal. Comparing Fig. 6 (e) and Fig. 7 (e), we can find that the amount of electron transfer in Fig. 7 (e) is about two times that in Fig. 6 (e). More electrons transfer from III to II is the most important factor for decreasing the work function. The direction of charge transfer is determined by the electronegativity of the element, as shown in [30], the electronegativity of molybdenum is 2.16 on the Pauling scale, and cesium is 0.79. So cesium always shows electropositive when close to the molybdenum. This means that the difference in electronegativity between atoms is also an important factor.

### 3.2. Cesium co-deposition with electronegative elements

Cesium is extremely low electronegative so cesium always loses its outermost electron and becomes positively charged when near an electronegative element as mentioned before. Although there is no reference report about the Fluorine atom in NBI, we have still chosen it in this work due to its strongest electronegative, and we hope that the F-Cs double-layer will enhance the charge transfer between the electropositive layer and the electronegative layer. Based on these reasons, we will discuss the double adsorption layers in consist of electropositive atoms (Cs) and electronegative atoms (H, C, O, and F). Compared with the works of C.A. Papageorgopoulos et al. [19–21], our models shown in Fig. 2 don't correspond to the minimum work function conditions for the Cs covered Mo/W with electronegative co-adsorbates. Rather than finding the minimum work function, we want to determine qualitatively the effect of co-adsorption on the work function and the dipole moment in this work. The ultimate goal of this work is to explore the physical mechanism of dipole moment change and finally the change of work function under the double-layer co-adsorption condition.

The work function is defined as the vacuum electrostatic potential minus the Fermi energy. We plot the electrostatic potential along the z-axis relative to Fermi energy ( $E_f = 0$ ) as shown in Fig. 8. We can see that whether it is Mo (110) or W (110) surface, the lowest work function is the case where Cs co-deposition with F and the F-Cs bond perpendicular to the surface (1.31 eV for Mo, and 1.23 eV for W). The second low is the O-Cs bond perpendicular to the surface for both Mo and W (1.54 eV for Mo, and 1.59 eV for W). The third is the H-Cs bond perpendicular to Mo (110) surface (1.85 eV) and the CCs bond perpendicular to the W (110) surface (1.62 eV). The fourth is the C-Cs bond perpendicular to Mo (110) surface (2.19 eV) and The HCs bond perpendicular to the W (110) surface (1.98 eV). We found that the work function is always going to be low as long as the bond is perpendicular to the surface, except for the C-Cs. There is little difference between the work function of co-deposition and that of pure cesium adsorption with the same coverage ( $\sigma = 0.34 \theta$ ) if the angle between the bond and surface is  $\alpha$  (2.18 eV for Mo and 2.28 eV for W, these values are in good agreement with the previous fit curve).

As shown in Fig. 9, the surface with H-Cs $_{\perp}$  has a large dipole moment compared with the bare surface and gives a lower work function (it's similar for C, O, and F). The  $p - p_0$  is consist of three components, including  $p_s - p_0$ ,  $p_a$ , and  $\Delta p$ . The restructuring of surface atoms induced by the additional H-Cs $_{\perp}$  group is similarly ignorable. Different from pure

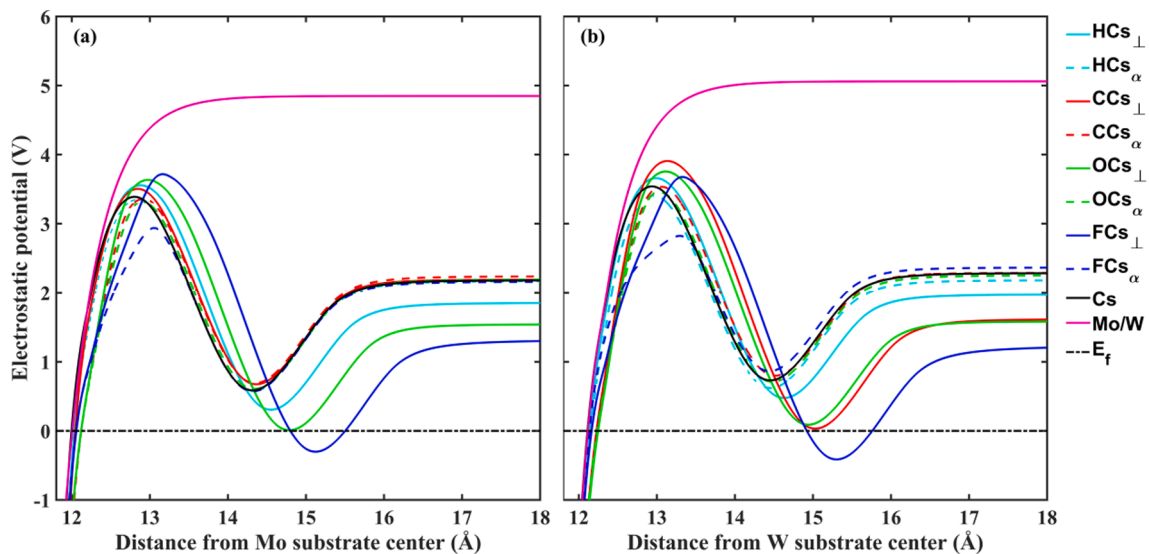
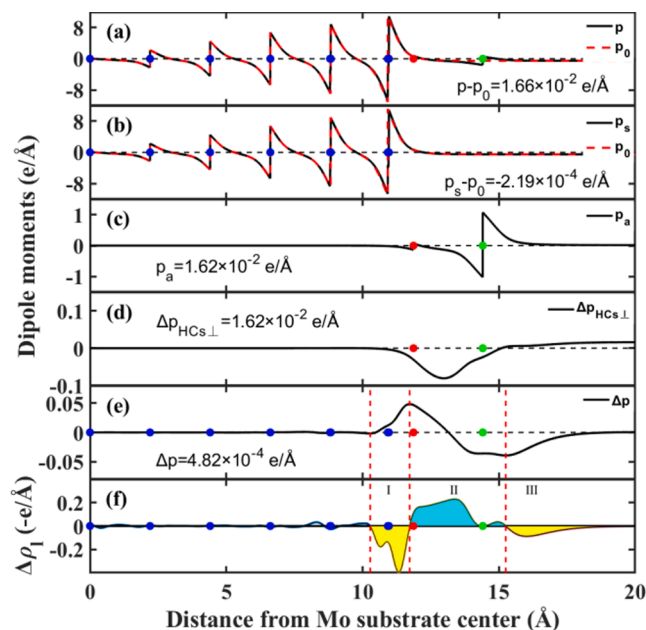


Fig. 8. The electrostatic potential relative to Fermi level of different surfaces: bare Mo (110) or W (110), Cs on Mo (W), and X-Cs on Mo (W), X represents H, C, O, or F.



**Fig. 9.** The H-Cs bond perpendiculars to Mo (110) surface. (a) The dipole moment density ( $p$ ) of “contaminative” Mo (110) surface and the dipole moment density ( $p_0$ ) of clean Mo (110) surface, the subscript means vertical, blue atoms represent the Mo layer, the red atom represents the H atom, and the green atom represents the cesium atom. (b) The dipole moment density ( $p_s$ ) of unrelaxing Mo (110) surface and  $p_0$ . (c) The intrinsic dipole moment of ( $p_a$ ) adsorbates. (d) The  $\Delta p_{\text{HCs}\perp}$  due to charge transfer between H and Cs. (e) The dipole moment density ( $\Delta p$ ) is due to electron transfer between adsorbates and the surface. (f) The electron density difference along the z-axis, the space near the surface is divided into 3 zones by the red dashed line, the yellow regions (I and III) represent electron depletion and the cyan region (II) represents electron accumulation. (For interpretation of the references to colour in this figure legend, the reader is referred to the web version of this article.)

cesium deposition,  $p_a$  makes a vital contribution to  $p - p_0$  and extremely matters. For an atom pair containing two atoms, like the H-Cs $_{\perp}$  group, its intrinsic dipole moment comes from the charge transfer between the electronegative element and the electropositive element. The  $p_a$  is also composed of three items, including the intrinsic dipole moment of the H atom and Cs atom and the dipole moment induced by charge transform between these two atoms. There are just two atoms within the H-Cs $_{\perp}$  group, and the intrinsic dipole moment for the single atom is zero as we have said above. So just the  $\Delta p_{\text{HCs}\perp}$  has a net contribution to the  $p_a$ . As shown in Fig. 9 (c) and (d), the  $p_a$  equals  $\Delta p_{\text{HCs}\perp}$ . Contrary to the pure cesium adsorption shown in Fig. 6, the role of  $\Delta p$  in this double-layer adsorption is very limited, or even sometimes counterproductive for decreasing work function ( $\Delta p$  is a negative value) as we observed in the case of O and F. This indicates the magnitude of electron transfer between the H-Cs $_{\perp}$  group and Mo (110) is very small. Even the electron will migrate towards the X-Cs $_{\perp}$ , if there is a very strong electronegative atom between cesium and substrate, like O and F. Although region II still gathers high electron density, more electrons come from region I not III, and as we said before it's not effective to decrease work function. The positive charges in region III are so small that the final  $\Delta p$  can't increase enough as shown in Fig. 9 (e) and (f). However, finally,  $p - p_0$  has a large enough value to reduce the work function because of the intrinsic dipole moment of H-Cs $_{\perp}$ . The main reason for Cs co-adsorption with F on Mo (110) or W (110) to obtain a very low work function is the electronegativity of F is too strong, and more electrons could be attracted from cesium and form a strong intrinsic dipole moment along the z-axis.

Unlike pure cesium deposition, there is an additional factor that can affect the dipole moment and then affect the work function. As shown in Fig. 8, the normal case has a smaller work function. The reason is the

projection of the intrinsic dipole moment of X-Cs in the z-direction will be larger.

As mentioned before, the tilted case is generally more stable than the normal case, we believe the tilted case is a more general situation in the negative ion source background.

We also calculated the work function of Cs co-deposition with H plasma on Mo(100) surface with different coverages as shown in Fig. 10. The ratio of H to Cs is 1:1 in this calculation. The surface structures of  $0.25\theta$ ,  $0.5\theta$  and  $1.0\theta$  are  $(2\sqrt{2} \times 2\sqrt{2}) - 45^\circ$ ,  $p(2 \times 2)$ , and  $c(2 \times 2)$ , respectively. For  $0.75\theta$ , the surface structure is combined with  $p(2 \times 2)$  and  $(4 \times 2)$  as the initial structure. The work function reaches the minimum at  $0.5\theta$  in both tilted (1.51 eV) and normal (1.48 eV) cases. And in most cases, normal adsorption has a smaller work function, except  $0.75\theta$ . The result of structure optimization of  $0.75\theta$  normal adsorption indicates there will be 2/3H-Cs groups that will change their normal state to tilt. The result of co-deposition indicates the H atom could further decrease the work function of cesiated surface during plasma discharge. The partial monolayer condition has a lower work function for both co-deposition and pure Cs deposition.

#### 4. Summary

We have calculated the work function of different cesiated surfaces with different cesium coverage and cesium co-deposition with the electronegative element by using the first-principles calculation based on density functional theory (DFT). We found that the minimum work function in pure cesium deposition occurs at a partial monolayer. The value of the minimum work function and corresponding coverage is different for various surfaces. The minimum work function of pure cesium deposition is 1.66 eV in our calculation and occurs at Mo (110) surface with a coverage  $\sigma = 0.56 \theta$ . The electron transfer is first increased and then inhibited with the increasing coverage of cesium. The work function of the double-layer adsorption depends on the angle between the bond and the surface and the electronegativity of the intermediate-layer atoms. The minimum work function of the double-layer occurs at the F-Cs bond perpendicular to W (110) surface, which is 1.23 eV. All these changes in work function are related to the changes in dipole moment density. A large dipole moment density is formed along the z-axis by depositing cesium on the substrate. This means that an additional electric field is formed in the opposite direction of the z-axis, which contributes to electron escape from the substrate. The double layer can further increase the dipole moment density due to the huge electronegativity difference. Although we get an extremely low work

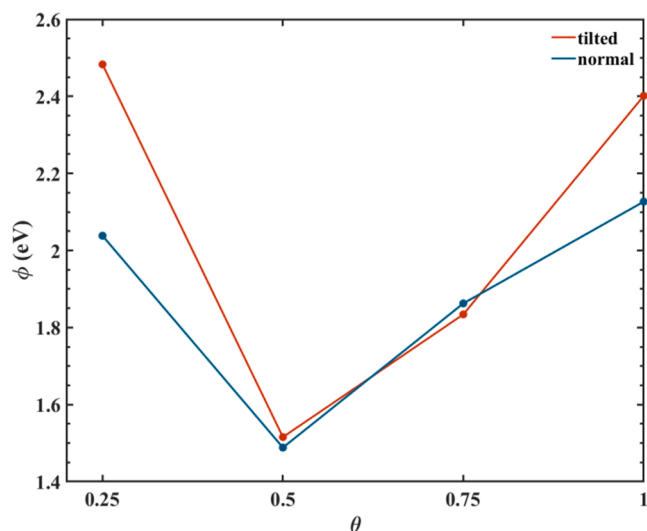


**Fig. 10.** The work function of Cs co-deposition with H plasma on the plasma grid.

function in this simulation work. We have to say, however, that the best situation is hard to occur in the harsh negative ion source background. We can also come out with an opposite prediction according to the physical mechanism, this work function may be extremely increased if the impurity particle is above the cesium. It relies on the specific environment, the type, and the quantity of impurity. Especially for negative ion sources, even if other impurities can be reduced by vacuuming or baking, hydrogen plasma is always present and necessary. According to the result of Cs co-deposition with H plasma on the plasma grid (Fig. 10), the minimum work function at least can reach about 1.5 eV. The smallest value is not necessarily achieved at 0.5 layers, depending on the minimum distinguishable interval of the surface adsorption density. No matter how this work just proposes an explanation and potential and idealized possibility of forming a double-layer to further reduce the work function of the plasma grid.

### CRedit authorship contribution statement

**Heng Li:** Conceptualization, Methodology, Formal analysis, Validation, Investigation, Writing – original draft, Writing – review & editing, Visualization. **Xin Zhang:** Conceptualization, Supervision, Funding acquisition, Software. **Yuhong Xu:** Supervision, Funding acquisition, Software. **Guangjiu Lei:** Conceptualization, Supervision, Funding acquisition. **Katsuyoshi Tsumori:** Conceptualization, Supervision, Validation, Writing – review & editing. **Mitsutaka Isobe:** Supervision, Validation. **Akihiro Shimizu:** Supervision, Validation. **Zilin Cui:** Validation, Investigation. **Yiqin Zhu:** Validation. **Jun Hu:** Validation. **Yuxiang Ni:** Supervision, Validation. **Shaofei Geng:** Conceptualization, Supervision, Validation. **Haifeng Liu:** Supervision, Validation. **Xianqu Wang:** Supervision, Validation. **Jie Huang:** Supervision, Validation. **Hai Liu:** Supervision, Validation. **Jun Cheng:** Supervision, Validation. **Changjian Tang:** Supervision, Validation. **CFQS team:** Supervision, Validation.

### Declaration of Competing Interest

The authors declare that they have no known competing financial interests or personal relationships that could have appeared to influence the work reported in this paper.

### Data availability

Data will be made available on request.

### Acknowledgments

This work was supported by the Natural Science Foundation of Sichuan Province (No.2022NSFSC0331), Sichuan International Science and Technology Innovation Cooperation Project (2021YFH0066), National Key R&D Program of China (2022YFE03070000, 2022YFE03070002).

### References:

- [1] K. Tsumori, K. Ikeda, H. Nakano, M. Kasaki, S. Geng, M. Wada, K. Sasaki, S. Nishiyama, M. Goto, G. Seriani, P. Agostinetti, E. Sartori, M. Brombin, P. Veltri, C. Wimmer, K. Nagaoka, M. Osakabe, Y. Takeiri, O. Kaneko, Negative ion production and beam extraction processes in a large ion source (invited), *Rev. Sci. Instrum.* 87 (2016) 02B936.
- [2] S. Masaki, H. Nakano, M. Kasaki, Y. Haba, K. Nagaoka, K. Ikeda, Y. Fujiwara, M. Osakabe, K. Tsumori, Spatial distribution of negative ion density near the plasma grid, *Rev. Sci. Instrum.* 91 (2020), 013512.
- [3] M. Bacal, M. Wada, Negative hydrogen ion production mechanisms, *Appl. Phys. Rev.* 2 (2015).
- [4] J.J.C.G. J.N.M Van Wunnik, E.H.A. Granneman, J. Los, The scattering of hydrogen from a cesiated tungsten surface, *Surf. Sci.* 131 (1983).
- [5] R. Gutser, C. Wimmer, U. Fantz, Work function measurements during plasma exposition at conditions relevant in negative ion sources for the ITER neutral beam injection, *Rev. Sci. Instrum.* 82 (2011), 023506.
- [6] U. Fantz, R. Gutser, C. Wimmer, Fundamental experiments on evaporation of cesium in ion sources, *Rev. Sci. Instrum.* 81 (2010) 02B102.
- [7] J.B. Taylor, I. Langmuir, The Evaporation of Atoms, Ions and Electrons from Caesium Films on Tungsten, *Phys. Rev.* 44 (1933) 423–458.
- [8] M. Seidl, H.L. Cui, J.D. Isenberg, H.J. Kwon, B.S. Lee, S.T. Melnychuk, Negative surface ionization of hydrogen atoms and molecules, *J. Appl. Phys.* 79 (1996) 2896–2901.
- [9] A. Krylov, D. Boilson, U. Fantz, R.S. Hemsworth, O. Provitina, S. Pontremoli, B. Zaniol, Caesium and tungsten behaviour in the filamented arc driven Kamaboko-III negative ion source, *Nucl. Fusion* 46 (2006) S324–S331.
- [10] A. Damone, A. Panarese, C.M. Coppola, J. Jansky, C. Coletti, L. Chiodo, G. Seriani, V. Antoni, S. Longo, Theoretical determination of the microstructure of Cs covering of Mo in negative ion sources for nuclear fusion applications, *Plasma Phys. Controlled Fusion* 57 (2015).
- [11] M. Rutigliano, A. Palma, N. Sanna, Hydrogen scattering from a cesiated surface model, *Surf. Sci.* 664 (2017) 194–200.
- [12] P. Singh, M. Bandyopadhyay, Role of angular orientation of dipoles on work function during cesium deposition on a metal surface – A phenomenological model, in: *AIP Conference Proceedings*, 2018.
- [13] T.C. Leung, C.L. Kao, W.S. Su, Y.J. Feng, C.T. Chan, Relationship between surface dipole, work function and charge transfer: Some exceptions to an established rule, *Phys. Rev. B* 68 (2003).
- [14] M. Khazaei, M. Arai, T. Sasaki, A. Ranjbar, Y. Liang, S. Yunoki, OH-terminated two-dimensional transition metal carbides and nitrides as ultralow work function materials, *Phys. Rev. B* 92 (2015).
- [15] M. Wada, Plasma-surface interaction in negative hydrogen ion sources, *Rev. Sci. Instrum.* 89 (2018), 052103.
- [16] L. Schiesko, C. Hopf, P. Franzen, W. Kraus, R. Riedl, U. Fantz, A study on backstreaming positive ions on a high power negative ion source for fusion, *Nucl. Fusion* 51 (2011).
- [17] P. Bharathi, A.J. Deka, M. Bandyopadhyay, M. Bhuyan, K. Pandya, R.K. Yadav, H. Tyagi, A. Gahlaut, A. Chakraborty, Study on production and extraction of negative impurity ions in a caesiated negative ion source, *Nucl. Fusion* 60 (2020).
- [18] A. Palma, N. Sanna, M. Rutigliano, Evidence of superoxide-like CsO<sub>2</sub> formation on a cesiated model surface, *Appl. Surf. Sci.* 534 (2020).
- [19] J.M.C.C.A. Papageorgopoulos, Coadsorption of electropositive and electronegative elements: II. Cs and O<sub>2</sub> on W(100), *Surf. Sci.* 39 (1973) 313–332.
- [20] J.M.C.C.A. Papageorgopoulos, Coadsorption of electropositive and electronegative elements: I. Cs and H<sub>2</sub> on W(100), *Surf. Sci.* 39 (1973) 283–312.
- [21] M.-K.-L. Ernst-Vidalis, C. Papageorgopoulos, The effects of Cs on the adsorption of H<sub>2</sub> on Mo(110), *Surf. Sci.* 276 (1987) 189–190.
- [22] J.E. Ortega, R. Miranda, Growth of K, Rb and Cs on Gaas(110), *Appl. Surf. Sci.* 56–8 (1992) 211–217.
- [23] P. Singh, M. Bandyopadhyay, K. Pandya, M. Bhuyan, A. Chakraborty, Characterization of in situ work function and cesium flux measurement setup suitable for cesium seeded negative ion source applications, *Nucl. Fusion* 59 (2019).
- [24] G. Kresse, J. Hafner, Ab initio molecular dynamics for liquid metals, *Phys. Rev. B Condens Matter.* 47 (1993) 558–561.
- [25] P. Hohenberg, W. Kohn, Inhomogeneous Electron Gas, *Phys. Rev.* 136 (1964) B864–B871.
- [26] J.P. Perdew, K. Burke, M. Ernzerhof, Generalized gradient approximation made simple, *Physical Review Letters*, 78 1997 1396–1399.
- [27] P.E. Blochl, Projector augmented-wave method, *Phys. Rev. B Condens Matter.* 50 (1994) 17953–17979.
- [28] P.E. Blochl, O. Jepsen, O.K. Andersen, Improved tetrahedron method for Brillouin-zone integrations, *Phys. Rev. B Condens Matter.* 49 (1994) 16223–16233.
- [29] H.J. Monkhorst, J.D. Pack, Special points for Brillouin-zone integrations, *Phys. Rev. B* 13 (1976) 5188–5192.
- [30] W.M. Haynes, *CRC handbook of chemistry and physics - 97th edition*, CRC press, 2016.